CERN-ACC-NOTE-2018-073
23-11-2018
corinna.martinella@cern.ch

Radiation levels in the LHC during the 2015 Pb-Pb and 2016 p-Pb run and mitigation strategy for the electronic systems during HL-LHC operation

Corinna Martinella[1], *Cristina Bahamonde Castro*[2], *Anton Lechner*[2], *Salvatore Danzeca*[3], *Yacine Kadi*[1], *Markus Brugger*[1], *Rubén Garcia Alia*[2]

[1]EN/EA, CERN, Geneva, Switzerland
[2]EN/STI/BMI, CERN, Geneva, Switzerland
[3]EN/SMM/RME, CERN, Geneva, Switzerland

Abstract

During the Pb-Pb and p-Pb operations of LHC, high localized beam losses can induce a risk of failure for the electronic systems installed in the tunnel. In the framework of the Radiation to Electronics Project (R2E), the radiation levels in the LHC were measured during the 2015 Pb-Pb and 2016 p-Pb runs and used to benchmark the available FLUKA Monte Carlo simulations, in order to predict the risk of failure for the future HL-LHC operation.

Keywords: Radiation levels in the LHC, R2E, Pb-Pb run, p-Pb run.

Contents

1 Introduction

During the 2015 Pb-Pb and 2016 p-Pb runs, high localized beam losses were measured in the Large Hadron Collider (LHC). Although the origin and the locations of these losses were different during the two operations, they similarly represent a risk for the electronic equipment installed in the tunnel.
In the framework of R2E, sets of active and passive measurements were carried out in the dispersion suppressors (DS) of IP1 and IP5 and compared with the available FLUKA Monte Carlo simulations for the implementation of the orbit bumps during the 2015 Pb-Pb run. The results allowed estimations for the future High Luminosity LHC (HL-LHC) radiation levels, when 3000 fb^{-1} are expected for the proton run ($\sim$100 times the luminosity in 2016) and 10 nb^{-1} for the ion run ($\sim$14 times the luminosity in 2015). Table 1 gives an overview of the luminosity integrated over the different periods [1] [10].

Table 1: Integrated Luminosity in 2015, 2016 and expected for HL-LHC.

		Luminosity			
Year	**Run**	**ATLAS (fb^{-1})**	**CMS (fb^{-1})**	**ALICE (nb^{-1})**	**LHCb (fb^{-1})**
2015	p-p	4.22	4.22	6.79	0.36
2016	p-p	38.49	40.96	13.39	1.88
2015	Pb-Pb	704 (μb^{-1})	600 (μb^{-1})	433 (μb^{-1})	7 (μb^{-1})
2016	p-Pb	39.32 nb^{-1} in ALICE at 8.16 TeV			
HL-LHC	p-p	3000 fb^{-1} in ATLAS/CMS			
HL-LHC	Pb-Pb	10 nb^{-1} in ALICE			

In this work, first an overview of the monitors and the simulations package used is given, then the Bound Free Pair Production (BFPP) mechanism, the results from the measurements and simulations and the mitigation strategies for the Pb-Pb run are presented for IP1, IP5 and IP2. The final chapter discusses on the loss pattern measured during the p-Pb run in 2016 and the associated risks for the electronics.

1.1 Layout

The LHC is about 26.7 km long. The ring is divided in 8 octants. Each octants starts from the middle of an arc and finishes at the middle of the following arc, containing 34 left and 34 right cells (see Figure 1). There are 8 Long Straight Sections (LSS: cell 1-7 left and right). The exact layout depends on the specific use of the insertion, e.g. beam collisions for physics (IR1, IR2, IR5, IR8), beam dumping (IR6), beam cleaning (IR3, IR7) or RF system (IR4). 16 Dispersion Suppressor (DS: cell 8-11) help in matching the insertion optics of the Long Straight Section to the periodic FODO solution of the arc (ARC: cell 12-34).

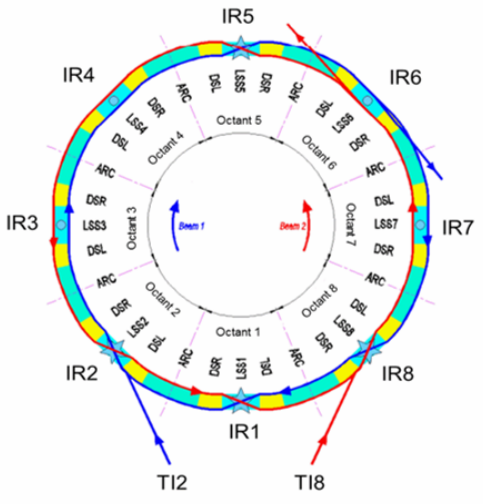

Fig. 1: Layout of the LHC: Long Straight Sections (LSS), Dispersion Suppressors (DS) and Arcs (ARC) are highlighted for the left (L) and right (R) sides.

2 Detectors and simulations

In this section, the monitors (BLMs, RADFET, RadMon) and simulation package (FLUKA) used in the work are shortly described.

Standard Beam Loss Monitoring (BLM) in the LHC are ionization chambers 50 cm long with a diameter of 9 cm and a sensitive volume of 1.5 liter, filled with N_2 at 100 mbar overpressure.
The aim of the BLM System is to protect the super-conducting magnets from quenching by generating a beam dump when the detected losses exceed certain thresholds. The BLMs are installed outside the cryostat at the beam line or on the top of the magnet at the interconnection. They allow the measurements of the energy deposited by secondary particle shower, giving the integrated dose as result. Furthermore, by measuring the loss pattern, the BLM system enables the identification of loss mechanisms in the LHC.

Radiation sensitive Field Effect Transistors (RadFET) are p-channel MOSFETs optimized for monitoring the Total Ionizing Dose (TID) on electronic devices. The incident radiation causes increasing of the positive trapped charges in the gate silicon oxide layer and a consequent shift in the voltage threshold as a function of the dose. The RadFETs used for this campaign were 400 nm oxide thickness, optimized for a medium sensitivity of 0.05 Gy and an optimal annual TID measurement range between 20-400 Gy [2]. During the Pb-Pb run in 2015, several passive RadFETs were installed directly under the cryostat in the high losses regions (see section 3.4).

The Radiation Monitoring System (RadMon V5) was developed at CERN in the EN Department. It is used to monitor the three important quantities to quantify the damage on the electronics.
Each RadMon V5 has 9 radiation sensors installed on board: 2 RadFETs with different oxide thickness (between 100 nm, 400 nm and 1000 nm) are used for the active Total Ionizing Dose (TID) measurements, 3 photodiodes in series to measure the 1 MeV equivalent neutron fluence for the Displacement Damage (DD) and a Toshiba SRAM memory to measure the cumulative High Energy Hadron (HEH) and thermal neutron fluence for the Single Event Effect (SEE), where with HEH are considered the hadrons with energy higher than 20 MeV [2]. $\sim$380 RadMons are installed in the underground areas of LHC.

FLUKA [3, 4] is a fully integrated particle physics Monte Carlo simulation package. Among other capabilities, it can accurately recreate beam-matter interactions taking place in particle accelerators such as the LHC. The code takes into account how particle showers develop after the beam reaches different accelerator components, and allows to quantify the relevant quantities needed to protect sensitive equipment. FLUKA is used to evaluate the risk for electronics in the tunnel, both when benchmarking current measurements of the aforementioned radiation monitors and when estimating future radiation levels. The relevant quantities to be recorded in FLUKA for this purpose are the dose to the BLMs and the dose and High Energy Hadron fluence in the RadFETs and RadMons, respectively.
A detailed model of the BLMs was included in the FLUKA geometry in each of the real BLM positions in the tunnel, allowing to record the dose in these locations. In a similar way, a mesh was placed underneath the cryostats in the FLUKA geometry of the DS covering the RadFET and RadMon positions and recording both dose and High Energy Hadron fluence. The mesh extended below all cryostats of the DS, with a height of 30 cm and 100 cm laterally. The mesh resolution was 50 cm longitudinally, 50 cm laterally and 30 cm in height. FLUKA simulations were performed for Pb-Pb runs to see the effects on IP1, IP5 and IP2, as is thoroughly described in the following sections.

3 Ion-Ion run 2015: IP1, IP5, IP2

3.1 Bound-Free Pair Production (BFPP)

During the Pb-Pb collisions the majority of pair-creation events do not change the state of the ions. However, there is a small fraction in which a quasi-real photon converts into an electron-position pair and the electron is trapped in one of the atomic shells of one ion.

$$^{208}Pb^{82+} + {}^{208}Pb^{82+} \longrightarrow {}^{208}Pb^{82+} + {}^{208}Pb^{81+} + e^{+} \quad (1)$$

This bound-free pair production (BFPP) has a cross-section of 281 barn (at 7 Z TeV) and results in the change of the magnetic rigidity of the ion. Consequently, the Pb^{81+} ions form well-defined secondary beams emerging from each side of the IP, much higher than the losses generated by the luminosity debris [5].

3.2 Mitigation strategies

Due to the high and localized power that BFPP beams carry, they can potentially cause a quench in the superconducting magnets installed in the DS at both sides of each interaction point. In IP8 the luminosity is too low for this to be a concern, but not in the rest of the IPs where mitigation strategies are needed.

During the Pb-Pb run at the end of 2015, orbit bumps were introduced in the DS around IP1 and IP5 to reduce this risk. By displacing and spreading out the losses, it has been shown that the orbit bumps were essential and will be so in future operations. Active and passive measurements were used to benchmark the FLUKA simulations and the results are shown in section 3.4. Moreover, the secondary beams produced by the BFPP effect were used to induce a controlled quench of a dipole magnet, providing the first direct measurement of steady state quench level [5].

In IP2, a similar strategy involving orbit bumps can not be implemented because optics are different and an orbit bump like those of IP1 and IP5 would not shift the BFPP losses to a connection cryostat. For 2015 operation, IP2 had a lower luminosity compared to IP1/IP5 so a quench was not expected, but to allow the ALICE experiment to operate at the luminosity foreseen in the 2020s, several mitigation strategies were evaluated using FLUKA [6] [7].
It was concluded that new collimators need to be installed in half-cell 11 of IR2 to intercept the BFPP beams. This needed a throughout evaluation of the expected consequences including a quench risk and cryogenics evaluation as well as an estimate of the risk to the electronics in this area. An orbit bump of 2.5 mm would also be needed in order to shift the BFPP losses to the collimator location.

FLUKA was used to evaluate the damage the concerned electronic racks (in half-cell 12 of the DS) could experience over the whole HL-LHC operation. The damage was quantified through the cumulative dose and the possibility of experiencing Single Event Effects through the High Energy Hadron fluence. At the end of the HL-LHC era, an integrated luminosity of 10 nb^{-1} is expected in the ALICE experiment, so all results were normalized to this value as can be seen in Figure 2.
Both plots show the longitudinal profile along the magnet below which the most exposed racks are. The figures display the exact rack locations as in the current LHC and the total dose and fluence, together with the contribution from BFPP to these totals.
Both the dose and HEH fluence display a strong gradient longitudinally, what would mean that shifting the racks towards the end of the magnet would halve the dose and fluence it would be exposed to.
Nevertheless, even implementing this shift in the racks, the R2E project recommends keeping the dose to less than 20 Gy per year for the current envisaged lifetimes. Since this would not be possible, a rack rotation or a non-electronic zone is foreseen for these areas of IR2.
In terms of HEH fluence, no risk of compromising the machine operation was found for distributed systems, since the probability of SEE failure may increase in these racks but not in the rest of the LHC, keeping the overall probability of failure unaffected.

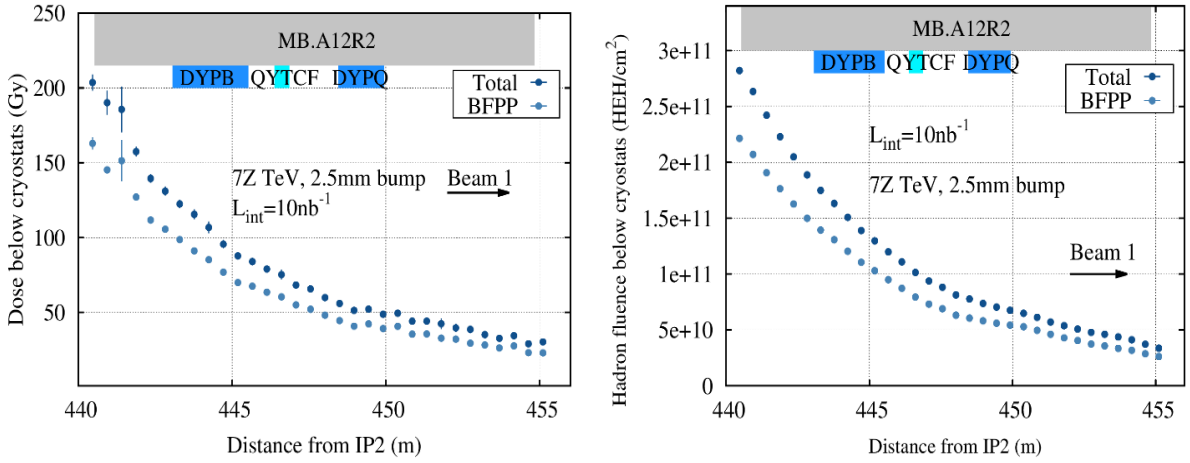

(a) Dose (b) HEH Fluence

Fig. 2: Dose and HEH fluence over the whole HL-LHC period expected below cryostats of cell 12 of the IR2 DS after the collimators are installed.

3.3 PbPb vs pp losses

The orbit bumps were introduced around IP1 and IP5 and the secondary beams generated by the BFPP effect were measured in cell 11 left and right side (11L1, 11R1, 11L5, 11R5). These losses reached peaks of few hundreds Gy, almost 100 times the annual baseline for the protons operation. The BLM measurements of dose during the entire protons and ions operations of 2015 are compared and shown in Figure 3.

The profile is the same looking at the measurements for the RadMons installed in cells 11L1, 11R1, 11L5, 11R5. In Figure 5 (a) are reported the Single Event Upset (SEU) counts in the SRAM memories generated by the HEH and the thermal neutrons. In Figure 5 (b) the TID measurements are shown for the two RadFETs installed on the board, where TID 1 represents the measurements from the 100 nm RadFET and the TID 2 the measurements from the 400 nm ones. It is clearly visible that during the p-p operations only few SEU or Gy were measured, while the profile increased sharply at the end of the year, when the operations moved from protons to Pb ions.

The HEH fluence and the TID measurements integrated over the entire protons and ions operations are listed in Table 2. It has to be noticed that not all the RadMon are installed in the same position respect to the cell structure, as reported in Appendix A. This has to be considered when comparing the measurements in different cells.

Finally in Figure 4 are shown the BLM measurements in IP2 for cell 10-11-12 . The levels are dominated by the ions run, reaching a peak of 302 Gy in cell 10 of the right side.

Table 2: RadMon dose Measurements in 2015

		p-p 2015		***Pb-Pb 2015***	
Cell	**Distance IP (m)**	**HEH Fluence HEH/cm^2**	**TID 2 (Gy)**	**HEH Fluence HEH/cm^2**	**TID 2 (Gy)**
11L1	432.8	4.40E+09	4.18	5.17E+10	49.15
11R1	432.1	7.14E+09	1.45	8.80E+10	14.04
11L5	433.5	5.15E+09	4.62	2.45E+10	21.97
11R5	425.5	5.41E+09	1.37	2.68E+11	58.74

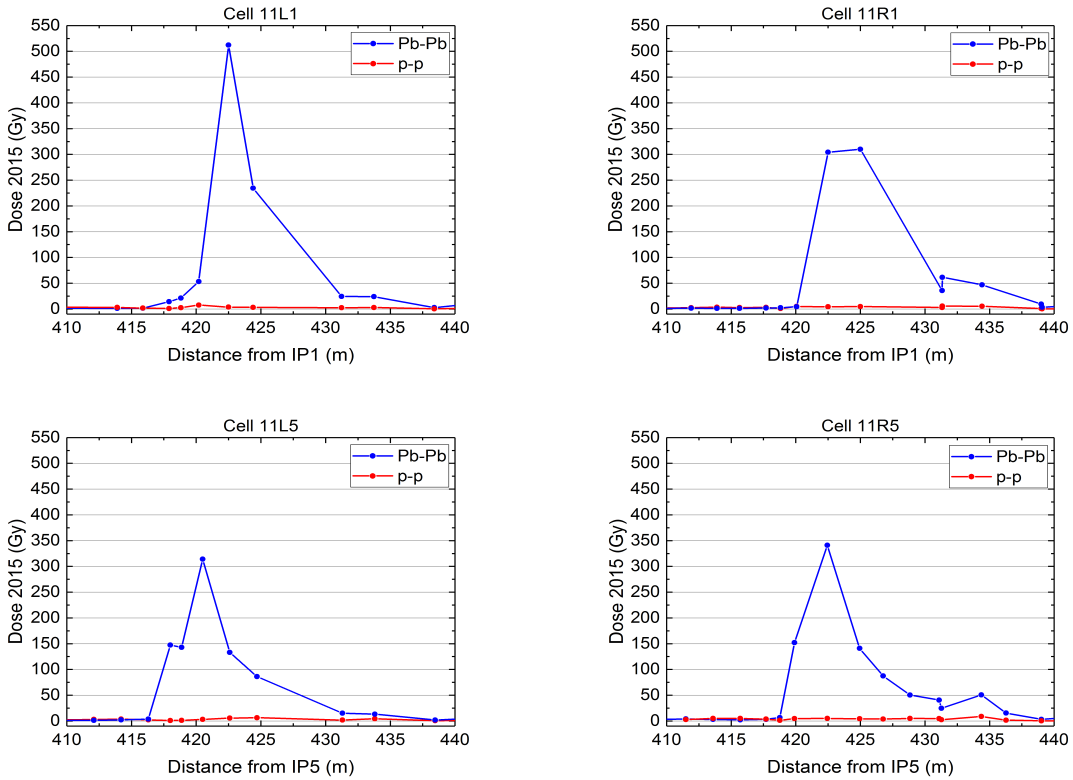

Fig. 3: BLM measurements in IP1 and IP5 during the p-p and the Pb-Pb run in 2015.

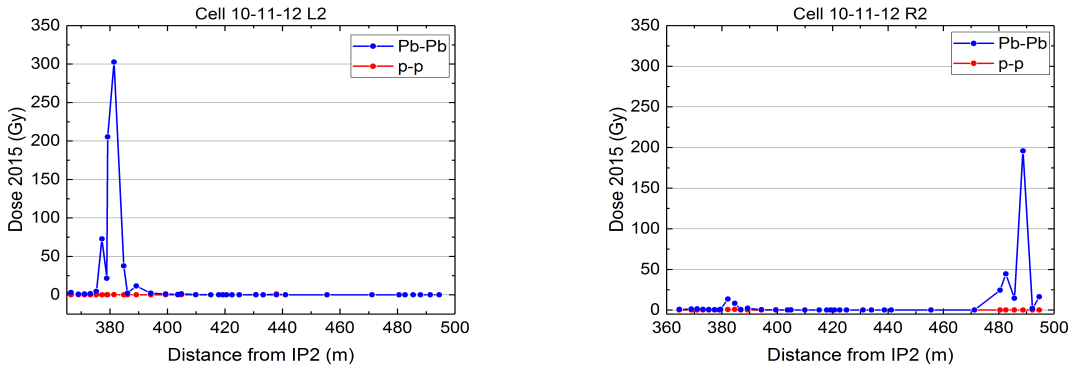

Fig. 4: BLM measurements in IP2 during the p-p and the Pb-Pb run in 2015.

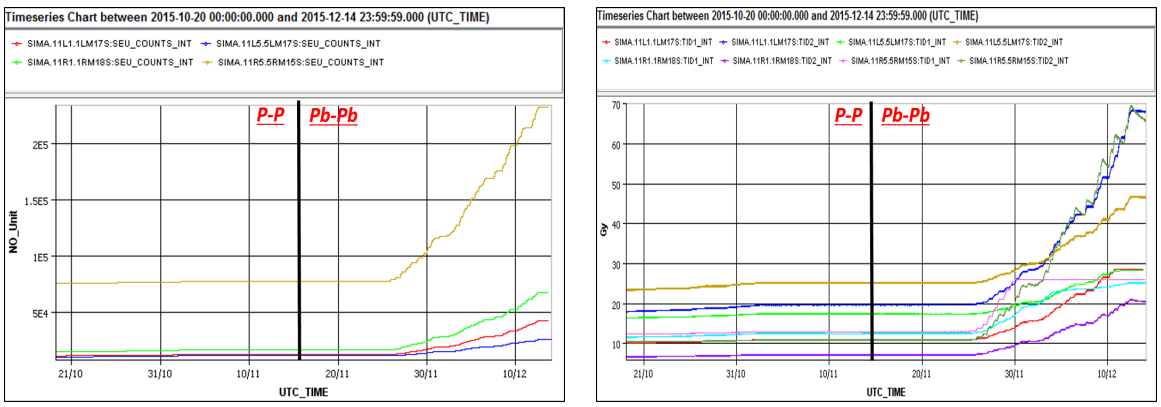

(a) SEU (b) TID

Fig. 5: RadMon measurements in cell 11 of IP1 and IP5 for the entire 2015: (a) Single Event Upset (SEU) counts from the SRAM memories, (b) TID measurements from 100 nm RadFETs (TID 1) and 400 nm ones (TID 2).

3.4 IP1 and IP5

In order to benchmark the FLUKA simulations of the orbit bumps, several passive RadFET were installed directly under the cryostat in cell 11L1 and 11R5. In this section all the different available sets of measurements are compared with the FLUKA simulations. The results and the locations of the passive RadFET are visible in Figure 6 for 11R5 and Figure7 for 11L1.

Between the simulated and the measured peaks there is a shift of -1.627 m in cell 11R5 and 1.997 m in cell 11L1. In both the comparisons, the contribution of the uncertainty over the passive RadFET positions and orbit bump has to be considered.

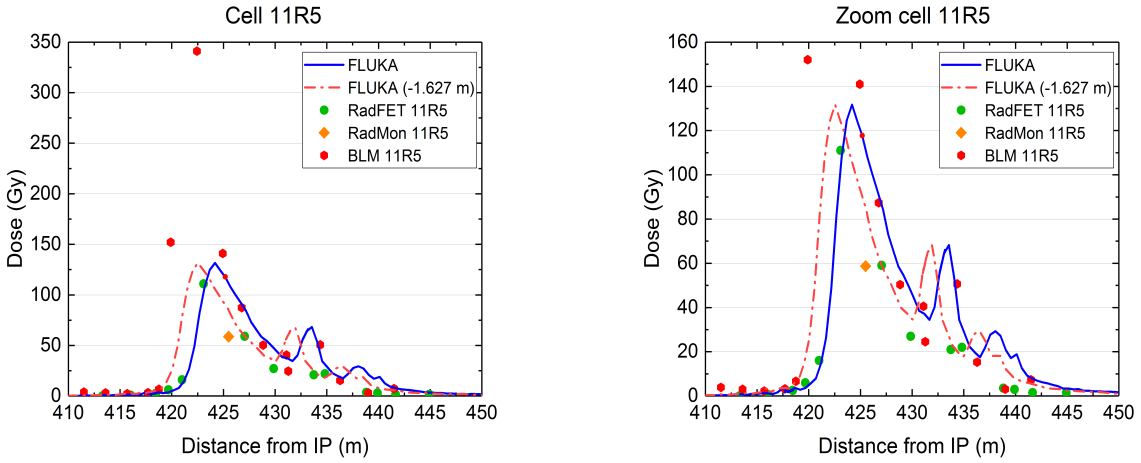

(a) (b)

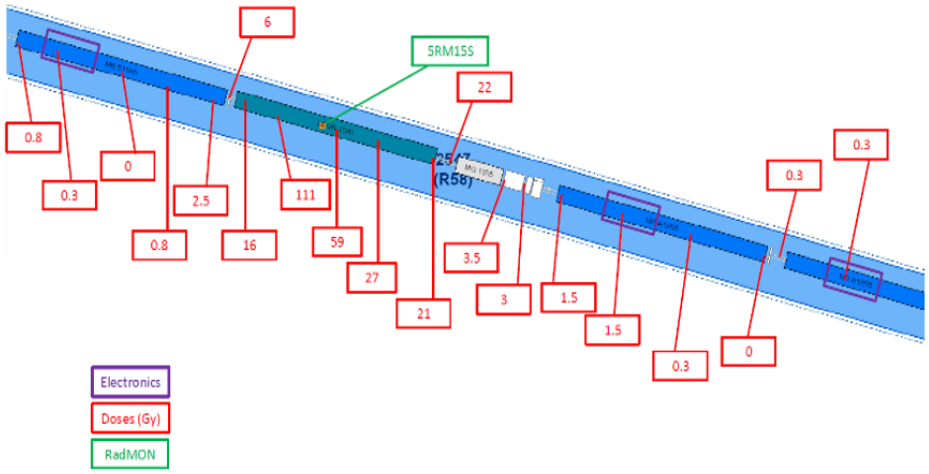

(c)

Fig. 6: (a) Comparison between the measurements in 11R5. (b) Zoom of the comparison. (c) Passive RadFET positions and TID measurements.

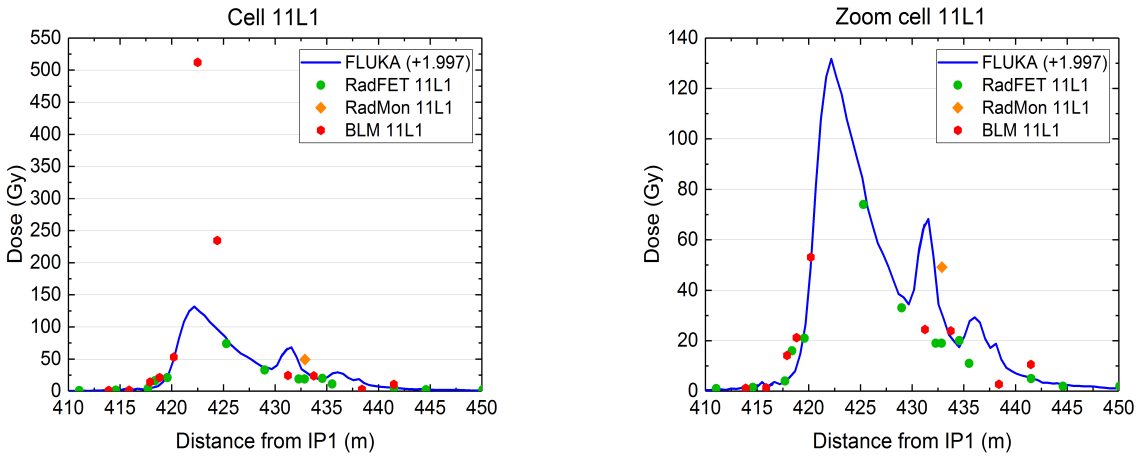

(a) (b)

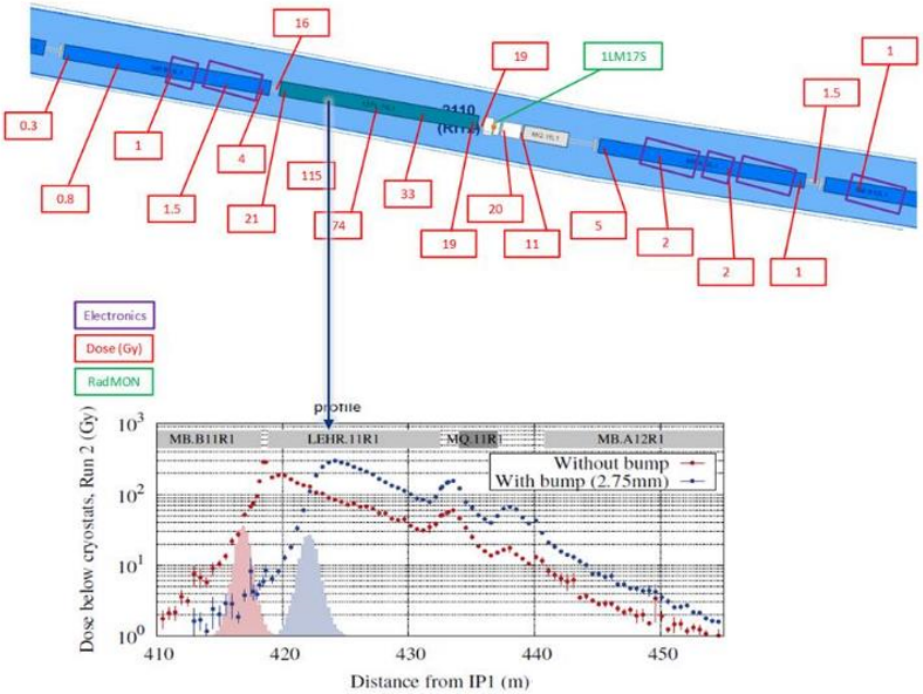

(c)

Fig. 7: (a) Comparison between the measurements in 11L1. (b) Zoom of the comparison. (c) Passive RadFET positions, TID measurements and FLUKA simulations profile.

4 Proton-Ion run 2016

The pilot Proton-Ion run was performed in 2012 and the first full one-month run in early 2013 [8]. The second full proton-nucleus run of the LHC took place in late 2016.

The collision of unequal beams requires a special "cogging" procedure since protons and lead circulate at slightly different speeds. During the "cogging", the beams are pushed transversely, onto opposite-sign off-momentum orbits, and longitudinally, to restore collisions at the proper interaction points after their rotation around the ring during the energy ramp [9] [10]. The colliding bunches have different sizes and charges. Furthermore, the two beams are created from different ion sources and this needs a complex bunch filling schemes in the LHC ring. This led to a particular loss pattern around the ring.

Compared to the 2015 Pb-Pb run, the peaks in cell 11 disappeared but, similarly, new peaks were detected in cell 8 close to the experiments. These peaks were not caused by the BFPP effect, but from fragments generated during the collisions in the experimental caverns.

Figure 8 shows the comparison of BLM measurements in cells 8 close to IP1 and IP5 (8L1, 8R1, 8L5, 8R5) during the different operations in 2015 and 2016. Two peaks were detected in all the 4 cells during the p-Pb run in 2016: one higher at ∼305 m and a lower at ∼296 m.
The RadMon measurements in Figure 9 confirm the increase in SEU counts and TID for the p-Pb operation at the end of 2016. Moreover, it is possible to notice that when the injection scheme changed and the ions switched from one beam to the other, also the loss pattern changed from left to right.
During the p-Pb run in 2016, some failures from the QPS were detected in B8L8 and B9R1. They were probably caused by the localized peaks measured in cell 8.

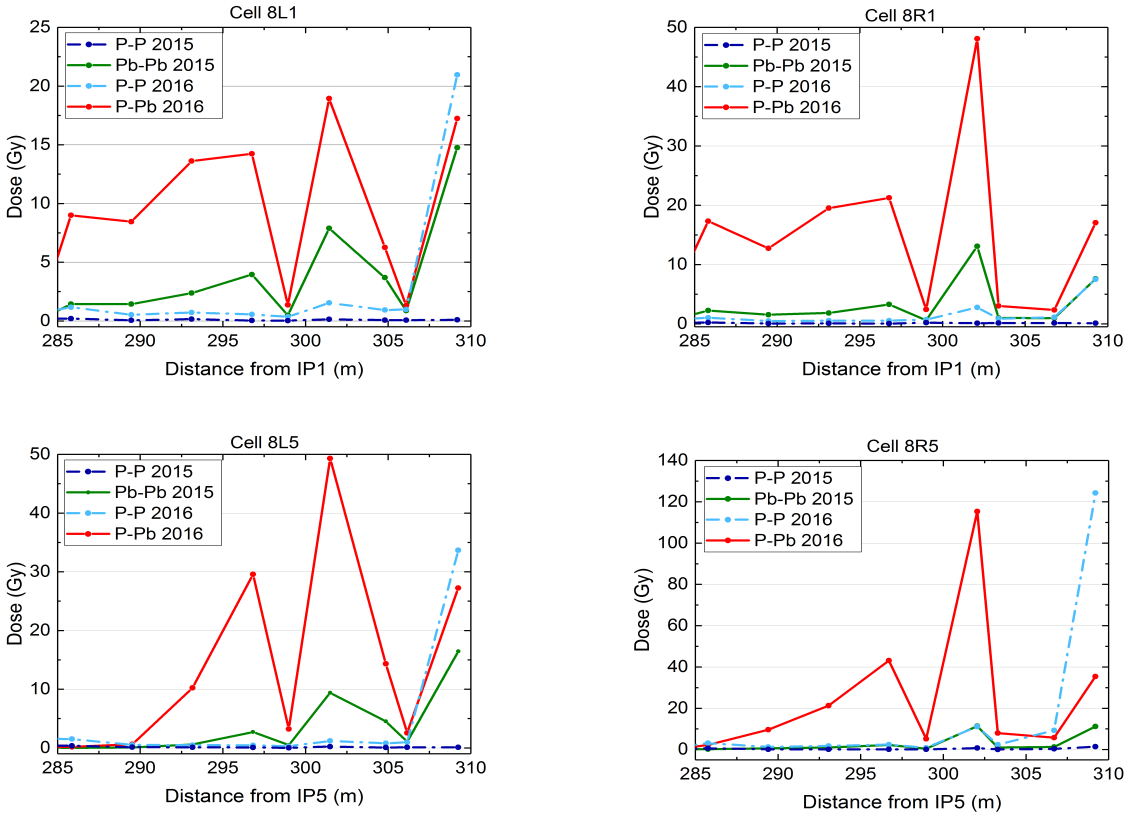

Fig. 8: BLM Dose measurements in cell 8 close to IP1 and IP5 (different y-axis scale).

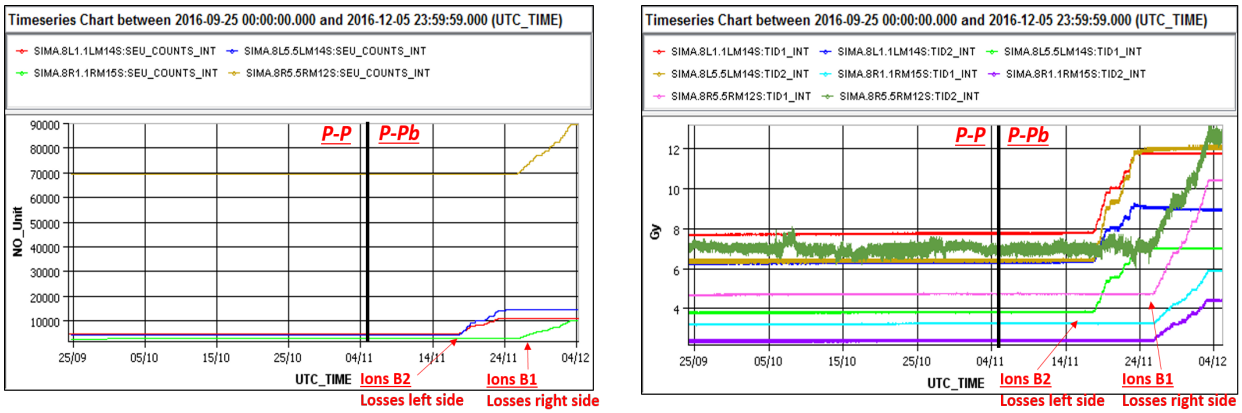

(a) SEU (b) TID

Fig. 9: RadMon measurements in cell 8 of IP1 and IP5 during the 2016 run: (a) Single Event Upset (SEU) counts from the SRAM memories, (b) TID measurements from 100 nm RadFETs (TID 1) and 400 nm ones (TID 2).

Figure 10 reports the BLM measurements for cells 8 close to IP2 and IP8. In both left and right side of IP2, two peaks are measured for the p-Pb run: at ∼302 m and ∼310 m distance.
Concerning IP8, in both sides there is a peak between ∼300 m and ∼305 m during the p-Pb run (as in the other IPs), but higher values were measured with protons in 2016.
The RadMon in IP2 measured as well a strong increase in the SEU count and TID during the p-Pb run at the end of 2016 operation. The results in Figure 11 refer to right side of IP2, since no RadMon are installed in the left side of IP2 and in cells 8 of point IP8.

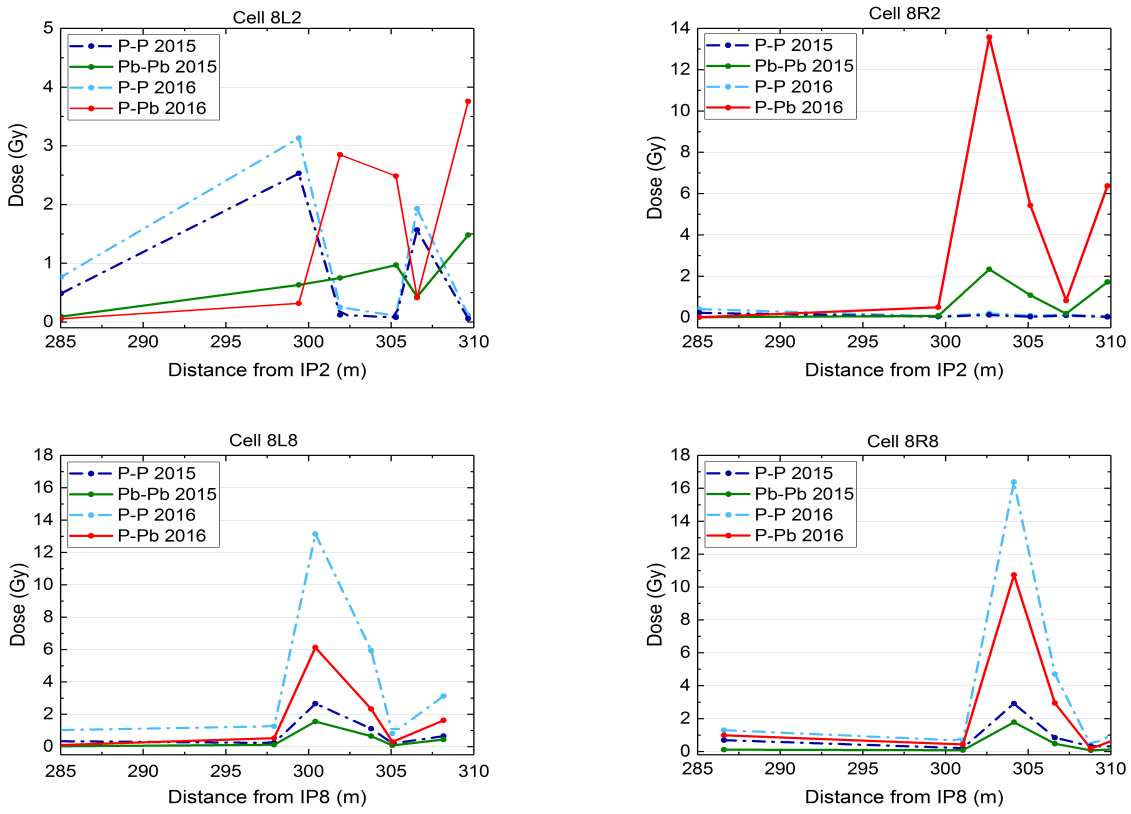

Fig. 10: BLM dose measurements in cell 8 close to IP2 and IP8 (different y-axis scale).

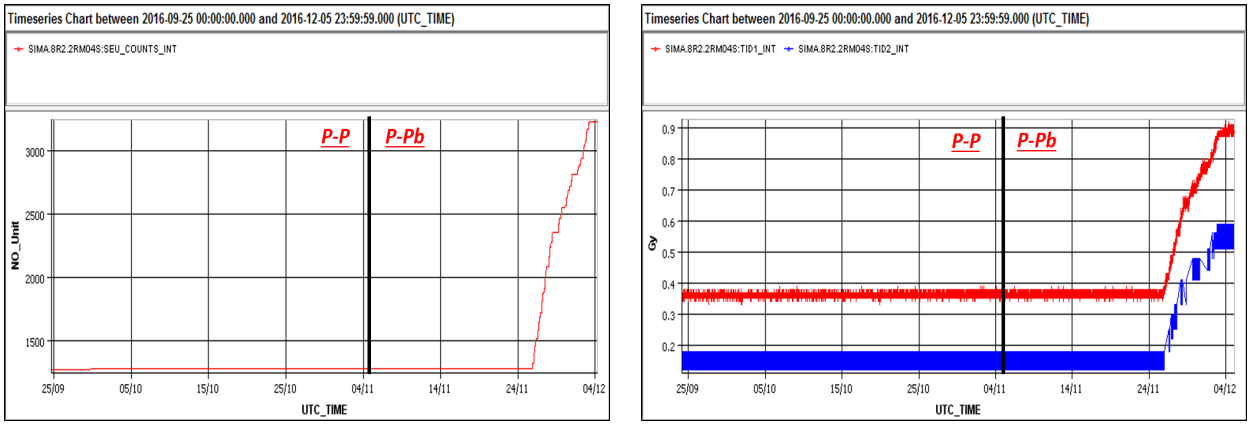

(a) SEU (b) TID

Fig. 11: RadMon measurements in cell 8 right side IP2 during the 2016 run: (a) Single Event Upset (SEU) counts from the SRAM memories, (b) TID measurements from 100 nm RadFETs (TID 1) and 400 nm ones (TID 2).

5 Conclusions

During the Pb-Pb run at the end of 2015, orbit bumps were introduced in the dispersion suppressors around IP1 and IP5 to mitigate the quench risk caused by the BFPP effect. This demonstrated that the orbit bumps will be essential in the future operations. Moreover, a controlled quench of a dipole magnet was induced by the secondary beams created by the BFPP effect, showing the need to install new dispersion suppressor collimators around IP2 to allow ALICE experiment to operate at the luminosity foreseen in the 2020s operations. FLUKA Monte Carlo simulations were performed for the orbit bumps in IP1 and IP5 and compared with different sets of measurements, showing a good agreement.
FLUKA was also used to evaluate the damage that electronic racks in IR2 DS could undergo by the end of HL-LHC as a consequence of installing a collimator in this area. The overall probability of SEE failure was found to be unaffected, but to keep the annual dose lower than 20 Gy as recommended by the R2E project, a rack rotation or non-electronic zone is foreseen for these areas of IR2.
Localized losses, higher than the p-p baseline, were also measured during the p-Pb operation, at the end of 2016. Two failures were detected in the QPS system and were probably induced by debris generated during the collisions. However, the p-Pb operation is an uncommon run and it will not be performed in LHC before 2028.
In conclusion, as first approximation for the radiation levels expected for HL-LHC, the contribution from the p-Pb operation can be considered negligible, while a scaling of $\sim$x10-14 for IP1 and IP5 can be applied for the ion run (10 nb^{-1} expected for HL-LHC vs 0.7 nb^{-1} accumulated in 2015). The contribution of the p-p run needs to be included as well and a scaling of $\sim$x100 can be applied in this case (3000 fb^{-1} expected for HL-LHC vs $\sim$39 fb^{-1} accumulated in 2016).

6 Acknowledgements

The authors would like to thank the Monitoring Calculation Working Group (MCWG) and all the people who participated in the measurements campaign. O. Stein and K. Bilko are gratefully acknowledged for their contribution on the BLMs measurements analysis.

7 References

[1] CERN, Accelerator Performance and Statistics, https://acc-stats.web.cern.ch/acc-stats/#lhc/.

[2] G. Spiezia et al., "The LHC radiation monitoring system RadMon", PoS (2011): 024.

[3] T.T. Böhlen, F. Cerutti, M.P.W. Chin, A. Fassó, A. Ferrari, P.G. Ortega, A. Mairani, P.R. Sala, G. Smirnov and V. Vlachoudis, "The FLUKA Code: Developments and Challenges for High Energy and Medical Applications", Nuclear Data Sheets 120, 211-214 (2014).

[4] A. Ferrari, P.R. Sala, A. Fasso, and J. Ranft, "FLUKA: a multi-particle transport code", CERN-2005-10, (2005).

[5] J.M. Jowett et al., "Bound-Free Pair Production in LHC Pb-Pb operation at 6.37Z TeV per Beam", IPAC2016, Busan, Korea.

[6] C. Bahamonde Castro et al., "Power Deposition in LHC Magnets Due to Bound-Free Pair Production in the Experimental Insertions", IPAC2016, Busan, Korea.

[7] C. Bahamonde Castro et al., "Needs for shielding in the connection cryostats in IR2 DS", 14th HL-LHC Technical Coordination Committee.

[8] J.M. Jowett et al., "Proton-Nucleus Collisions in the LHC", Proc. 4th Int. Particle Accelerator Conf. IPAC2013, Shanghai, China, May 2013.

[9] J.M. Jowett et al., "The LHC as a Proton-Nucleus Collider", in Proc. EPAC'06, Edinburgh, Scotland, 2006.

[10] J.M. Jowett et al., "The 2016 proton-nucleus run of the LHC", Proceedings of IPAC2017, Copenhagen, Denmark.

Appendices

A RadMons location in the tunnel

A.1 Cell 11: IP1, IP5 and IP2

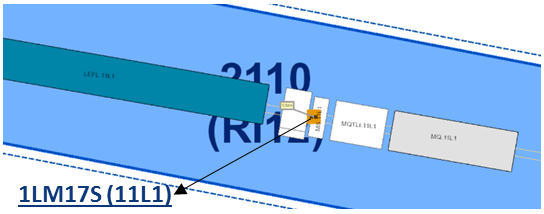

(a) 11L1

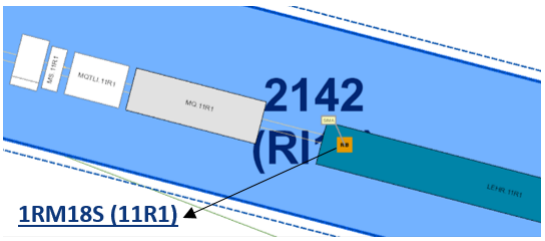

(b) 11R1

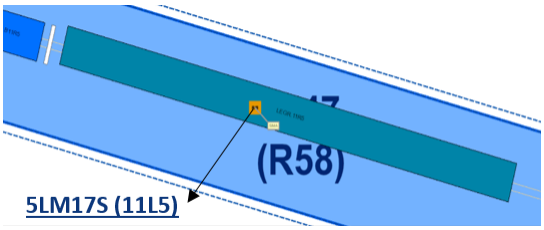

(c) 11L5

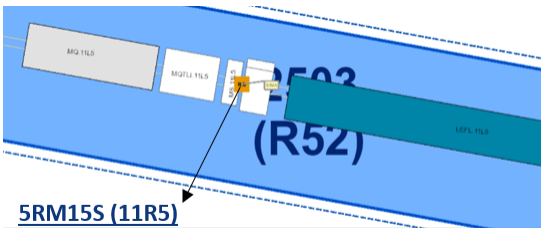

(d) 11R5

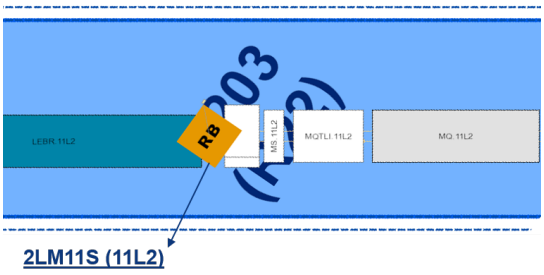

(e) 11L2

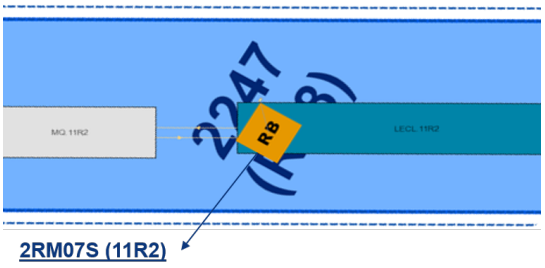

(f) 11R2

A.2 Cell 8: IP1, IP5

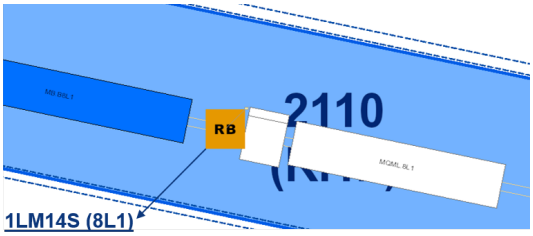

(a) 8L1

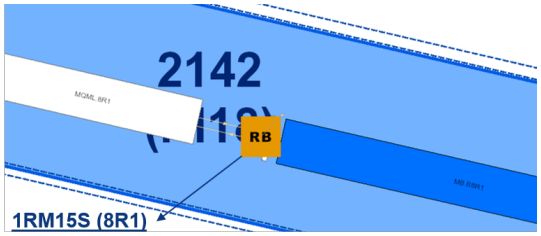

(b) 8R1

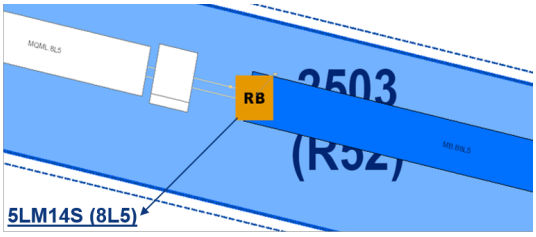

(c) 8L5

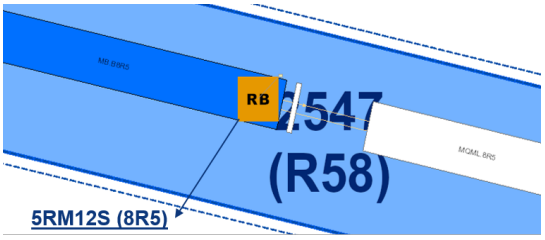

(d) 8R5